Demonstration of quantum permutation parity determine algorithm in a superconducting qutrit

Kunzhe Dai(戴坤哲), Peng Zhao(赵鹏), Mengmeng Li(李蒙蒙), Xinsheng Tan(谭新生), Haifeng Yu(于海峰), Yang Yu(于扬)

What follows is a list of articles you may be interested in

Frequency-tunable transmon in a three-dimensional copper cavity

Pan Jia-Zheng, Cao Zhi-Min, Fan Yun-Yi, Zhou Yu, Lan Dong, Liu Yu-Hao, Chen Zhi-Ping, Li Yong-Chao, Cao Chun-Hai, Xu Wei-Wei, Kang Lin, Chen Jian, Yu Hai-Feng, Yu Yang, Sun Guo-Zhu, Wu Pei-Heng
Chin. Phys. B . 2015, 24(11): 110301. **doi:** 10.1088/1674-1056/24/11/110301

Nonlocal multi-target controlled—controlled gate using Greenberger–Horne–Zeilinger channel and qutrit catalysis

Chen Li-Bing, Lu Hong
Chin. Phys. B . 2015, 24(7): 070307. **doi:** 10.1088/1674-1056/24/7/070307

Thermal quantum and total correlations in spin-1 bipartite system

Qiu Liang, Ye Bin
Chin. Phys. B . 2014, 23(5): 050304. **doi:** 10.1088/1674-1056/23/5/050304

Realization of quantum Fourier transform over Z_N

Fu Xiang-Qun, Bao Wan-Su, Li Fa-Da, Zhang Yu-Chao
Chin. Phys. B . 2014, 23(2): 020306. **doi:** 10.1088/1674-1056/23/2/020306

Correlation dynamics of two-parameter qubit-qutrit states under decoherence

Yuan Hao, Wei Lian-Fu
Chin. Phys. B . 2013, 22(5): 050303. **doi:** 10.1088/1674-1056/22/5/050303

Demonstration of quantum permutation parity determine algorithm in a superconducting qutrit[*]

Kunzhe Dai(戴坤哲)[1], Peng Zhao(赵鹏)[1], Mengmeng Li(李蒙蒙)[1], Xinsheng Tan(谭新生)[1,†],

Haifeng Yu(于海峰)[1,2,‡], and Yang Yu(于扬)[1,2]

[1] *National Laboratory of Solid State Microstructures, School of Physics, Nanjing University, Nanjing 210093, China*

[2] *Synergetic Innovation Center of Quantum Information & Quantum Physics, University of Science and Technology of China, Hefei 230026, China*

A quantum algorithm provides a new way in solving certain computing problems and usually faster than classical algorithms. Here we report an implementation of a quantum algorithm to determine the parity of permutation in a single three-dimensional (3D) superconducting transmon qutrit system. The experiment shows the capacity to speed up in a qutrit, which can also be extended to a multi-level system for solving high-dimensional permutation parity determination problem.

Keywords: quantum algorithm, qutrit, superconducting quantum computing

PACS: 03.67.Ac, 03.67.Lx, 85.25.–j   **DOI:** 10.1088/1674-1056/27/6/060305

1. Introduction

Quantum computation has been fascinating as the great potential power in solving the computational tasks more efficiently than the classical computer.[1] Over the past few decades, lots of quantum algorithms[2,3] have been proposed and provide a new vision in solving certain problems. Most of the quantum algorithms can realize quantum intrinsic parallel computation in a system with at least two entangled qubits, e.g., the Deutsch-Josza algorithm,[4] Shor's factoring algorithm,[5] Grover's searching algorithm,[6] and so on.[7–10] Generally, superposition and entanglement are considered as the main sources of acceleration of quantum computation. Mark Howard *et al.*[11] proposed that quantum contextuality[12] also plays an important role in determining the power of quantum computing; although the origin of the speed-up in quantum algorithms has been studied a lot, it is still not completely clear.[13] Recently, an interesting and simple quantum algorithm[14,15] is proposed to realize computational speed-up and the implementation requires only a single qutrit. This quantum algorithm can determine the parity of permutation twice as fast as the classical algorithm. It has been experimentally demonstrated in different types of quantum systems, including the nuclear magnetic resonance systems[14,15] and optical systems.[16,17] As the single qutrit is the smallest system[18] where the quantum contextuality can be observed, these experiments support the points that the entanglement is not necessary in all quantum speed-up, and the contextuality may be the origin of the speedup in this algorithm.

As one of the most promising candidates for building a quantum computer, superconducting quantum circuits can also be used to realize this quantum algorithm. In superconducting quantum circuits, people usually use the lowest two levels of the transmon to serve as a qubit for designing quantum computation algorithms. However, it is well known that a single superconducting transmon actually possesses multiple energy levels and can be treated as an artificial atom. A multi-level system, which corresponds to a large Hilbert space, can not only be used to design a Hamiltonian for quantum simulations,[19,20] but also store or encode more quantum information,[21–25] so that it can perform a much more complicated quantum algorithm than a qubit. In this paper, we demonstrate the permutation algorithm in a superconducting 3D transmon qutrit, which is the simplest case to show the computational speed-up. Our scheme holds the promise to extend the permutation algorithm to *N* dimensions with *N* levels or *N* qubits, providing a platform for studying the origin of speed-up in a superconducting quantum circuit system.

2. Quantum permutation algorithm

Considering there is a black box to realize cyclic permutations, in the three objects case, the six different permutations can be defined in the set of $1, 2, 3$, which are $(1, 2, 3)$, $(2, 3, 1)$, $(3, 1, 2)$, $(3, 2, 1)$, $(2, 1, 3)$, and $(1, 3, 2)$. The parity of these permutations can be categorized as even or odd, depending on whether the number of the performed exchange operations would be even or odd. Therefore, the first three are even permutations and the last three are odd permutations. The com-

putational task is to determine the parity of the cyclic permutations realized by the black box after query. In the quantum setting, the input and the output are the qutrit state $|m\rangle$, where $m = 0, 1, 2$ denote the three energy levels of the qutrit. The permutation can be considered as a function $y = f(x)$ which maps the input $x \in 0, 1, 2$ to the output $y \in 0, 1, 2$. These permutation functions can be realized by the unitary transformation acted on the qutrit. The six permutation functions written in Cauchy's two-line notation and the corresponding unitary transformations are given in the Eq. (1) below.

$$
f_1 = \begin{pmatrix} 0 & 1 & 2 \\ 0 & 1 & 2 \end{pmatrix}, \quad U_1 = \begin{pmatrix} 1 & 0 & 0 \\ 0 & 1 & 0 \\ 0 & 0 & 1 \end{pmatrix},
$$

$$
f_2 = \begin{pmatrix} 0 & 1 & 2 \\ 1 & 2 & 0 \end{pmatrix}, \quad U_2 = \begin{pmatrix} 0 & 1 & 0 \\ 0 & 0 & 1 \\ 1 & 0 & 0 \end{pmatrix},
$$

$$
f_3 = \begin{pmatrix} 0 & 1 & 2 \\ 2 & 0 & 1 \end{pmatrix}, \quad U_3 = \begin{pmatrix} 0 & 0 & 1 \\ 1 & 0 & 0 \\ 0 & 1 & 0 \end{pmatrix},
$$

$$
f_4 = \begin{pmatrix} 0 & 1 & 2 \\ 2 & 1 & 0 \end{pmatrix}, \quad U_4 = \begin{pmatrix} 0 & 0 & 1 \\ 0 & 1 & 0 \\ 1 & 0 & 0 \end{pmatrix},
$$

$$
f_5 = \begin{pmatrix} 0 & 1 & 2 \\ 1 & 0 & 2 \end{pmatrix}, \quad U_5 = \begin{pmatrix} 0 & 1 & 0 \\ 1 & 0 & 0 \\ 0 & 0 & 1 \end{pmatrix},
$$

$$
f_6 = \begin{pmatrix} 0 & 1 & 2 \\ 0 & 2 & 1 \end{pmatrix}, \quad U_6 = \begin{pmatrix} 1 & 0 & 0 \\ 0 & 0 & 1 \\ 0 & 1 & 0 \end{pmatrix}.
$$

(1)

In the classical scheme, to determine the parity of permutations requires the query on the black box (function) for at least two different inputs. However, the quantum permutation algorithm has been proposed to solve this problem with only one step of query. In the quantum permutation algorithm, the initial state is prepared in the ground state $|0\rangle$ of the qutrit. By doing a qutrit quantum Fourier transformation (QFT)[1] defined as

$$
U_{QFT} = \frac{1}{\sqrt{3}} \begin{pmatrix} \exp-\dfrac{2\pi i}{3} & \exp\dfrac{2\pi i}{3} & 1 \\ \exp\dfrac{2\pi i}{3} & \exp-\dfrac{2\pi i}{3} & 1 \\ 1 & 1 & 1 \end{pmatrix},
$$

(2)

we transform the qutrit state into the superposition state

$$
|\psi_0\rangle = \frac{1}{\sqrt{3}}\left[\exp\left(-\frac{2\pi i}{3}\right)|0\rangle + \exp\left(\frac{2\pi i}{3}\right)|1\rangle + |2\rangle \right].
$$

Then the superposition state is sent into the black box. After the permutation operation (U_k or f_k, where $k = 1, 2, \ldots, 6$ labels the six permutations in Eq. (1)) in the back box, the state can be written as

$$
|\psi_1\rangle = U_k|\psi_0\rangle = \frac{1}{\sqrt{3}}\left[\exp\left(-\frac{2\pi i}{3}\right)|f_k(0)\rangle \right.
$$

$$
\left. + \exp\left(\frac{2\pi i}{3}\right)|f_k(1)\rangle + |f_k(2)\rangle \right].
$$

Finally, an inverse QFT is carried out and the final state can be measured. The total flow diagram of the algorithm is shown in Fig. 1. When the parity of the permutation is even ($k = 1, 2, 3$), we obtain the final state $|0\rangle$ with global phases 0, $\exp(\pm 2\pi i/3)$. For odd permutation ($k = 4, 5, 6$), the result state is $|1\rangle$ with global phases 0, $\exp(\pm 2\pi i/3)$. Thus, a single step of query is sufficient to determine the parity.

Fig. 1. (color online) The flow diagram of the quantum permutation algorithm. The black box contains an unknown permutation operation given in Eq. (1). Before and after the permutation, there is a QFT and inverse QFT operation which is different from the classical scheme.

3. Experimental details

The experiment system is a superconducting transmon embedded in a 3D aluminum cavity. The main purpose of the cavity in our experiments is to provide a clean electromagnetic environment and to serve as a convenient tool for manipulation and measurement.[19,26] The sample is an Al–AlO$_x$–Al Josephson junction about the size of 150 nm × 150 nm connected to two aluminum pads, which is fabricated on a sapphire substrate. The whole pattern is fabricated with e-beam lithography and double angle e-beam evaporation technique. Here we use the lowest three energy levels of the transmon, namely $|0\rangle$, $|1\rangle$, and $|2\rangle$, as a qutrit system. From spectroscopy measurement, we obtain the transition frequency between $|0\rangle$ and $|1\rangle$ is $\omega_{01} = 2\pi \times 7.1572$ GHz, and the transition frequency between $|1\rangle$ and $|2\rangle$ is $\omega_{12} = 2\pi \times 6.8154$ GHz. From these transition frequencies, we can calculate the anharmonicity of the qutrit $\alpha = 2\pi \times 341.8$ MHz. The relatively large anharmonicity ensures that the manipulation applied on any two level transitions would not cause other spurious excitations. The resonant frequency of the 3D cavity is $\omega_c = 2\pi \times 9.0524$ GHz. The coupling strength between the qutrit and the cavity is about $2\pi \times 50$ MHz. In our design, the detuning between the qutrit transition frequency and cavity frequency are much larger than the coupling strength between the qutrit and the cavity, thus the system works in the dispersive region.[27] The energy relaxation time T_1 of the qutrit is about 10 µs and the decoherence time T_2 measured from the Ramsey experiment is about 8 µs. The device is cooled in a cryogen-free dilution refrigerator to a base temperature of about 20 mK. The amplifiers and filters are used in our measurement circuit to increase the signal-to-noise ratio and isolate the device from external noise.

In our experiment setup, two microwave vector signal generators combined with four digital to analog converter (DAC) channels of an Arbitrary Wave Generator (AWG) of the model Tektronix 5014c is used to irradiate the transmon

qutrit on-resonance with the transition frequency ω_{01} and ω_{12} respectively. The four DAC channels generate square waveforms of different amplitudes and lengths for IQ (In-phase and Quadrature) mixers on the vector signal generators to realize a different XY rotation of the qutrit. The amplitude corresponding to the driving strength is firstly calibrated by the Rabi oscillation experiments. Another microwave source is used to read out the qubit states by measuring cavity transmission. Here we choose the "high power readout" scheme,[19] which provides sufficient noise-to-signal ratio of our data and simplifies our experiment procedures and data analysis. Figure 2 shows our experimental setup for manipulating the 3D transmon qutrit.
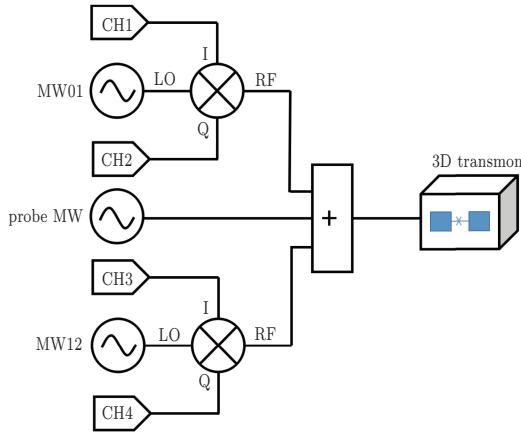

Fig. 2. (color online) Schematic diagram of experimental setup for manipulating a 3D superconducting transmon qutrit. The MW01 (MW12) source is used to drive the qutrit on-resonance with the transition frequency ω_{01} (ω_{12}). The DAC channels 1,3 (2,4) are used for manipulations along the x axis (y axis). Both driving microwave pulses and probe microwave pulse are sent into the device through a combiner.

4. Results

Initially, we prepared the qutrit on the ground state $|0\rangle$. The QFT is then implemented by a sequence of six selective rotation pulses $R_y^{01}(90°)$, $R_y^{12}(109.47°)$, $R_y^{12}(-90°)$, $R_x^{12}(-180°)$, $R_y^{12}(90°)$, and $R_y^{01}(-90°)$ as shown in Fig. 3. The selective rotation $R_\alpha^{mn}(\theta)$ denotes the rotation between qutrit basis states $|m\rangle$ and $|n\rangle$ along the axes α with the rotation angle θ. This combination has a factor $-i$ different from the QFT described in Eq. (2), which can be seen as a global phase, thus has no impact on the experiment result. The six unitary transformations that compose the permutation operations in the black box are also realized by the combination of different selective rotations. After the black box, an inverse pulse sequence of QFT is applied to realize the inverse QFT. In order to extract the complete information of the result, we employ the state tomography technique[28] to characterize the final state. As the final states are always projected on $|0\rangle$ and $|1\rangle$, being independent on whether the parity of the permutation is odd or even, we can consider the states $|0\rangle$ and $|1\rangle$ as the query register and the state $|2\rangle$ as the auxiliary state. Therefore, we can only perform the two level state tomography on

the query register, which simplifies the experiment and thus realize the quantum algorithm with a higher fidelity. Generally, the state of a two level system can be described with the density matrix $\rho = (1/2)I + (1/2)\boldsymbol{r} \cdot \hat{\boldsymbol{\sigma}}$, where I is the unit matrix, $\boldsymbol{r}$ is the state vector on the Bloch sphere, and $\hat{\boldsymbol{\sigma}}$ is the Pauli vector. We can reconstruct the density matrix completely by obtaining the information of state components along x, y, and z axes. In our experiment, we use the MW01 source in Fig. 2 whose frequency is on-resonance with the transition frequency ω_{01} to generate the tomography pulse sequence. By measuring populations in the states $|0\rangle$ and $|1\rangle$ after a selective rotation of angle $90°$ along the x and y axes on the Bloch sphere, we can obtain the x and y components of the final state, respectively. The z component can be directly readout without any additional rotation from the populations in the states $|0\rangle$ and $|1\rangle$.
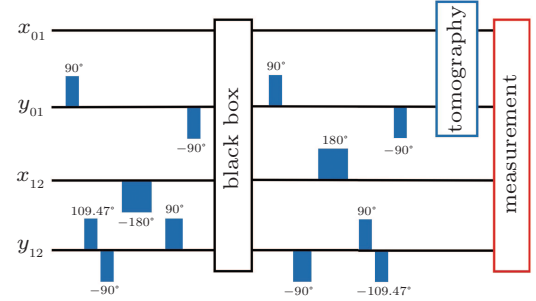

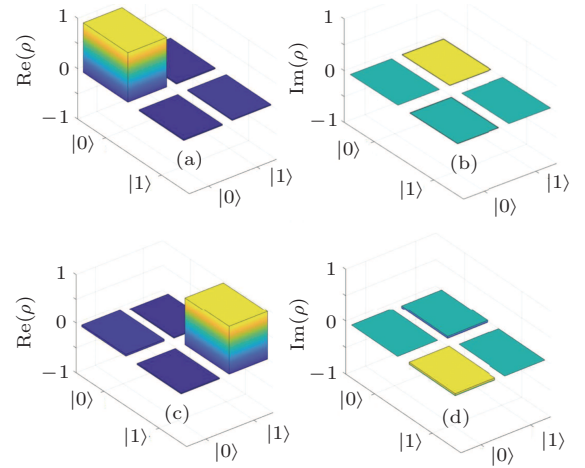**Fig. 3.** (color online) The total pulse sequence of experiment.

Fig. 4. (color online) The state tomography of the final state. Panels (a) and (b) ((c) and (d)) are the real and imaginary parts of the final state under the even (odd) permutation operation U_1 (U_4).

Figure 4 shows the results of our implementation of permutation algorithm, with panels (a) and (b) for the permutation U_1 and panels (c) and (d) for the permutation U_4. Following the principles discussed above, we reconstruct the density matrices (including the real (Re) and imaginary (Im) parts) of the final state. The results agree with the expectation, the U_1 operation can be determined as even permutation, while the U_4 operation can be determined as odd permutation. The fidelity we obtained is 0.9836 for the even permutation U_1 and 0.9641

for the odd permutation U_4. The fidelity of the other permutations U_2, U_3, U_5, and U_6 are 0.9049, 0.9086, 0.8392, and 0.8534, respectively. The final state resulting from each permutation is plotted on the Bloch sphere, which can be seen in Fig. 5.
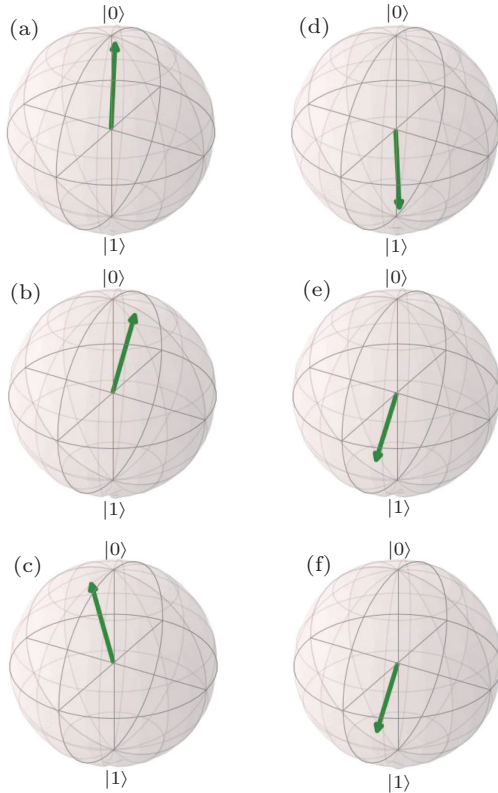

Fig. 5. (color online) The final state on the Bloch sphere. Panels (a), (b), and (c) correspond to the final state (predicted to be $|0\rangle$) resulting from the even permutation U_1, U_2, and U_3. Panels (d), (e), and (f) correspond to the final state (predicted to be $|1\rangle$) resulting from the odd permutation U_4, U_5, and U_6.

5. Conclusion

In this paper, we propose an experimental realization of the quantum permutation algorithm based on a 3D transmon qutrit and demonstrate the implementation of this algorithm to determine the parity of two permutations. The decoherence and the calibration imperfection are the main limits to the fidelity of our experiment, while the fidelity we obtained is still high enough to determine the parity of the permutations. Employing the third state of the transmon realizes the single step query speed-up in this experiment, which shows the potential power of a multi-level system in processing quantum information. This experiment also provides a possible way for theoretical discussion and exploring the origin of quantum speed-up.

References

[1] Nielsen M A and Chuang I L 2000 *Quantum Computation and Quantum Information* (Cambridge: Cambridge University Press)
[2] Montanaro A 2016 *npj Quantum Information* **2** 15023
[3] Cleve R, Ekert A, Macchiavello C and Mosca M 1998 *Proc. R. Soc. Lond. A* **454** 339
[4] Deutsch D and Jozsa R 1992 *Proc. R. Soc. Lond. A* **439** 553
[5] Shor P W 1997 *SIAM J. Comput.* **26** 1484
[6] Grover L K 1997 *Phys. Rev. Lett.* **79** 325
[7] Farhi E, Goldstone J, Gutmann S, Lapan J, Lundgren A and Preda D 2001 *Science* **292** 472
[8] Han K H, Kim J H 2000 *Proceedings of the Congress on Evolutionary Computation*, July, 2000, pp. 1354–1360
[9] Kassal I, Jordan S P, Love P, Mohseni M and Aspuruguzik A 2008 *Proc. Natl. Acad. Sci. USA* **105** 18681
[10] Ambainis A 2007 *SIAM J. Comput.* **37** 210
[11] Howard M J, Wallman J J, Veitch V and Emerson J 2014 *Nature* **510** 351
[12] Zhang X, Um M, Zhang J H ,An S M, Wang Y, Deng D L, Shen C, Duan L M and Kim K 2013 *Phys. Rev. Lett.* **110** 070401
[13] Den N and Maarten V *Phys. Rev. Lett.* 2013 **110** 060504
[14] Dogra S, Arvind and Dorai K 2014 *Phys. Lett. A* **378** 3452
[15] Gedik Z, Silva I A ,Cakmak B, Karpat G, Vidoto E L G, Soarespinto D O, Deazevedo E R and Fanchini F F 2015 *Sci. Rep.* **5** 14671
[16] Wang F R, Wang Y L, Liu R F, Chen D X, Zhang P, Gao H and Li F L 2015 *Sci. Rep.* **5** 10995
[17] Zhan X, Li J, Qin H, Bian Z H and Xue P 2015 *Opt. Express* **23** 18422
[18] Kochen S and Specker E P 1967 *J. Math. Mech.* **17** 59
[19] Tan X S, Zhao Y X, Liu Q, Xue G M, Yu H F, Wang Z D and Yu Y 2017 *npj Quantum Materials* **2** s41535
[20] Houck A, T´ureci H E and Koch J 2012 *Nat. Phys.* **8** 292
[21] Kiktenko E O, Fedorov A K, Manko O V and Manko V I 2015 *Phys. Rev. A* **91** 042312
[22] Kiktenko E O, Fedorov A K, Strakhov A A and Manko V I 2015 *Phys. Lett. A* **379** 1409
[23] Lanyon B P, Barbieri M, Almeida M P, Jennewein T, Ralph T C, Resch K J, Pryde G J, Obrien J L, Gilchrist A and White A 2009 *Nat. Phys.* **5** 134
[24] Muthukrishnan A and Stroud C R 2000 *Phys. Rev. A* **62** 052309
[25] Zhao J, Tan X S, Lan D, Wu H T, Xue G M, Yu H F and Yu Y 2017 *Phys. Status Solidi B* **254** 1600640
[26] Rigetti C, Gambetta J M, Poletto S, Plourde B L T, Chow J M, Córcoles A D, Smolin J A, Merkel S T, Rozen J R, Keefe G A, Rothwell M B, Ketchen M B and Steffen M 2012 *Phys. Rev. B* **86** 100506
[27] You J Q and Nori F 2003 *Phys. Rev. B* **68** 064509
[28] Bianchetti R, Filipp S, Baur M, Fink J M, Lang C, Steffen L, Boissonneault M, Blais A and Wallraff A 2010 *Phys. Rev. Lett.* **105** 223601